Alternating Phenylenevinylene Copolymers with Dithienbenzothiadiazole Moieties: Synthesis, Photophysical, and Photovoltaic Properties

John A. Mikroyannidis,[1] Minas M. Stylianakis,[1] Qingfeng Dong,[2] Jianing Pei,[2] Wenjing Tian[2]

[1]*Chemical Technology Laboratory, Department of Chemistry, University of Patras, Patras GR-26500, Greece*
[2]*State Key Laboratory of Supramolecular Structure and Materials, Jilin University, Changchun 130012, China*

Received 12 January 2009; accepted 9 April 2009
DOI 10.1002/app.30580
Published online 16 July 2009 in Wiley InterScience (www.interscience.wiley.com).

ABSTRACT: Two new soluble alternating phenylenevinylene copolymers **S** and **L** which contained dithienbenzothiadiazole moieties were synthesized by Heck coupling. The repeating unit of **L** was longer than that of **S** and contained two additional phenylene rings and two cyano-vinylene bonds. Both copolymers were stable up to about 350°C and afforded char yield of 52–66% at 800°C in N_2. Their absorption spectra were broad and extended up to about 600 nm with a longer wavelength maximum at 447–502 nm and optical band gap of $\sim$ 2.0 eV. These copolymers emitted yellow light in solution with PL maximum at 551–580 nm and orange-red light in thin film with PL maximum at 588–661 nm. The emission maximum of **L** was considerably red-shifted relative to **S**. Photovoltaic cells based on **S** (or **L**) as donor and [6,6]-phenyl C61-butyric acid methyl ester as acceptor were investigated. © 2009 Wiley Periodicals, Inc. J Appl Polym Sci 114: 2740–2750, 2009

Key words: conjugated polymers; synthesis; dithienbenzothiadiazole; photophysics; polymer solar cells; poly(*p*-phenylenevinylene); cyanovinylene

INTRODUCTION

Bulk heterojunctions fabricated by blending polymers with fullerene have resulted in great improvements in the polymer solar cells (PSCs) efficiencies. The most commonly used materials for the fabrication of bulk heterojunctions are poly(3-hexylthiophene) (P3HT) and PCBM.[1–9] With optimized device structure and fabrication conditions, P3HT/PCBM bulk heterojunction solar cells can reach efficiencies as high as 4.4–5.0%.[1–3] However, novel materials with lower energy gaps need to be developed to improve the coverage of the solar spectrum and consequently improve the efficiency.

Poly(*p*-phenylenevinylene)s (PPVs) are greenish-yellow light-emitting polymers.[10,11] Nevertheless, to be utilized in the single-layer LED devices with higher work function metal as the cathode, PPV has the drawback that it is a poor electron acceptor due to its high LUMO energy. To improve the electron injection ability of the polymers, abundant derivatives of PPV have been reported with electron-withdrawing substituents such as halide,[12–14] cyano,[15,16] trifluoromethyl,[17] or methylsulfonyl-phenyl[18] on the arylene rings. Other examples with electron-withdrawing groups on vinylene group of conjugated polymers have also been reported.[19-23] A power-conversion efficiency (n_p) value of 1% and IPCE (incident-photon-to-current conversion efficiency) of 6% at low light intensities have been reported for a bulk heterojunction-PV system formed from two different conjugated polymers: poly[2-methoxy-5-(2-ethylhexyloxy)-1,4-phenylene vinylene] (MEH-PPV) as the donor, in composite with cyano-PPV (CN-PPV) as the acceptor.[24] Recently, much higher IPCEs of 23,[25] 25,[26] and 30%[27] have been measured in PPV-based binary-blend devices with white-light efficiencies of 0.75[25] and 1.7%.[27]

At present, the optical band gaps (E_g^{opt}) of the substituted PPVs and the polythiophenes commonly used in the PSCs are typically 2.0–2.2 eV[28,29] and not optimized with respect to the solar spectrum (ca. 350–1500 nm).[30,31] Organic solar cells are a major driving force for research in band gap engineering. However, polymers with $E_g^{opt} > 2.0$ eV only absorb radiation in the UV and green part of the visible range. Therefore, chemists have been making efforts to synthesize new low-band gap polymers (i.e., polymers with $E_g^{opt} < 1.9$–2.0 eV) to harvest more photon energies at long wavelengths to increase the photocurrent. The low band gap can be achieved by incorporating alternating donor (D) and acceptor (A) moieties in the polymer main chains.[32–42] The basic

Correspondence to: J. A. Mikroyannidis (mikroyan@chemistry.upatras.gr).

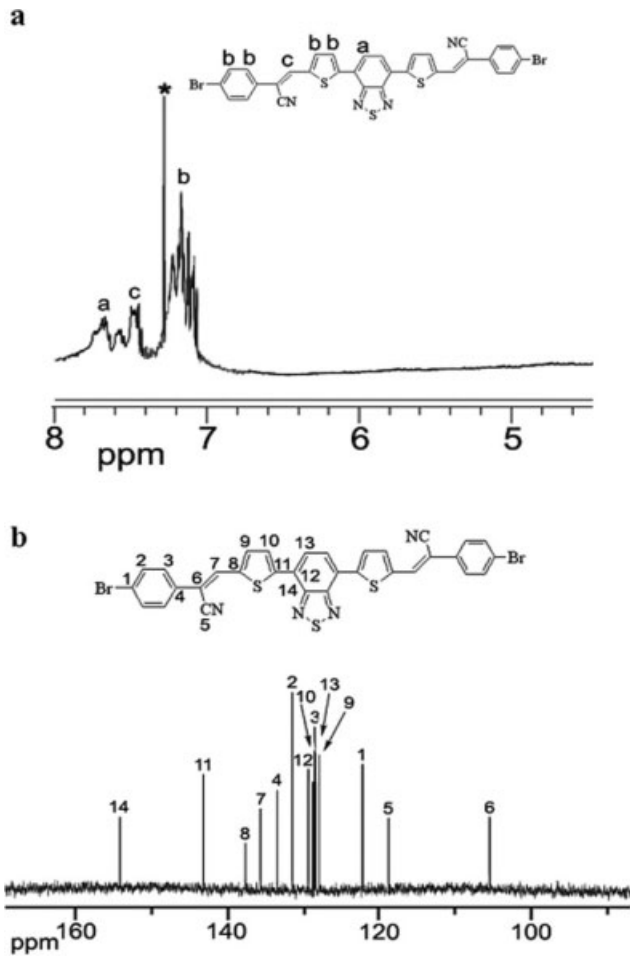

Figure 1 ^{1}H-NMR (a) and ^{13}C-NMR (b) spectra in $CDCl_3$ solution of the key-dibromide **6**. The solvent peak is denoted by an asterisk in the ^{1}H-NMR spectrum.

idea is that conjugated systems with a regular alternation of electron-rich donor and electron-deficient acceptor groups will exhibit a broadening of the valence and conduction bands and thus band gap reduction.[43-46] 2,1,3-Benzothiadiazole[43,47,48] and thiophene[49-51] derivatives have been widely used as π-conjugating spacers in push–pull chromophores designed for the production of low-band gap conjugated polymers.

The main objective of this investigation was the synthesis of two conjugated alternating phenylenevinylene copolymers **S** and **L** with dithienbenzothiadiazole moieties that could be used for photovoltaic cells. They were successfully prepared by Heck coupling and carried solubilizing hexyloxy side groups. The repeating unit of **L** was longer than that of **S** and contained cyano-vinylene bonds. The characteristic of these copolymers is that the vinylene bonds were incorporated between the electron-rich units (dihexyloxybenzene) and electron-deficient units (dithienbenzothiadiazole). The introduction of the cyano groups onto the PPV main chain is expected to lower the LUMO level of the copolymer. The thermal, photophysical, and photovoltaic properties of the copolymers were investigated and correlated with their chemical structures.

MATERIALS AND METHODS

Characterization methods

IR spectra were recorded on a Perkin-Elmer 16PC FTIR spectrometer with KBr pellets. ^{1}H-NMR (400 MHz) and ^{13}C-NMR (100 MHz) spectra were obtained by using a Bruker spectrometer. Chemical shifts (δ values) are given in parts per million with tetramethylsilane as an internal standard. UV–vis spectra were recorded on a Beckman DU-640 spectrometer with spectrograde THF. The PL spectra were obtained with a Perkin Elmer LS45 luminescence spectrometer. The PL spectra were recorded with the corresponding excitation maximum as the excitation wavelength. Thermogravimetric analysis (TGA) was performed on a DuPont 990 thermal analyzer system. Ground samples of about 10 mg each were examined by TGA and the weight loss comparisons were made between comparable specimens. Dynamic TGA measurements were made at a heating rate of 20°C/min in atmospheres of N_2 at a flow rate of 60 cm^3/min. Elemental analyses were carried out with a Carlo Erba model EA1108 analyzer.

Reagents and solvents

Tributyl-2-thienyl-stannane was prepared from the reaction of thiophene with *n*-BuLi in hexane and subsequently with tributylchlorostannane according to the literature.[52] 1,4-Divinyl-2,5-bis(hexyloxy)-benzene was synthesized by Stille reaction[53] of 1,4-dibromo-2,5-bis(hexyloxy)-benzene with tri-*n*-butyl-(vinyl)tin according to the literature.[54] *N,N*-Dimethylformamide (DMF) and tetrahydrofuran (THF) were dried by distillation over CaH_2. Triethylamine was purified by distillation over KOH. All other reagents and solvents were commercially purchased and were used as supplied.

Preparation of monomers

2,1,3-Benzothiadiazole (**1**)

Compound **1** was prepared from the reaction of 1,2-diaminobenzene with thionyl chloride in dichloromethane in the presence of triethylamine.[55]

4,7-Dibromo-2,1,3-benzothiadiazole (**2**)

Compound **2** was prepared by brominating **1** in aqueous hydrobromic acid.[55]

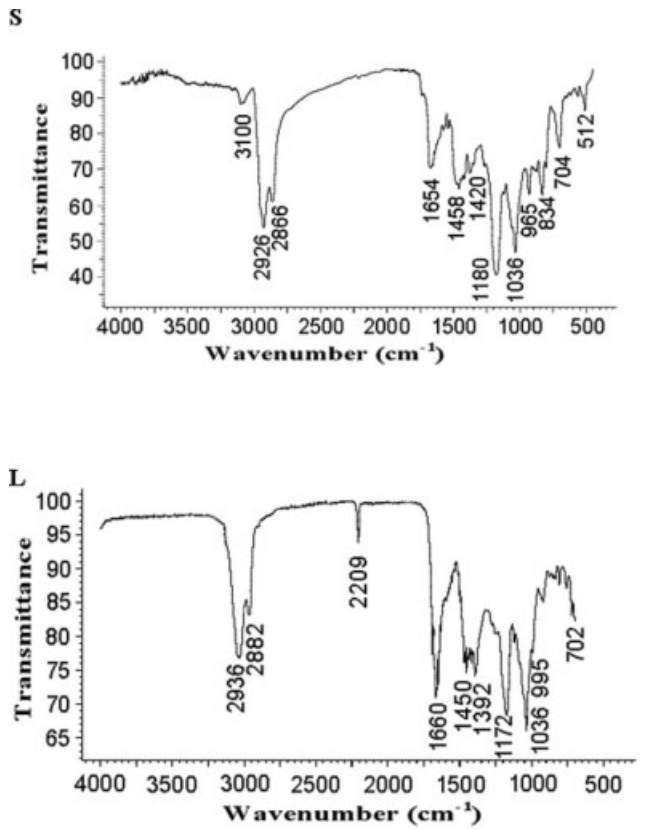

Figure 2 FTIR spectra of copolymers **S** (top) and **L** (bottom).

4,7-Di-2-thienyl-2,1,3-benzothiadiazole (**3**)

Compound **3** was prepared by coupling **2** with tributyl-2-thienyl-stannane in THF in the presence of $PdCl_2(PPh_3)_2$.[34]

4,7-Bis(5-bromo-2-thienyl)-2,1,3-benzothiadiazole (**4**)

Compound **4** was prepared from the reaction of **3** with *N*-bromosuccinimide in chloroform.[56]

5,5′-(2,1,3-Benzothiadiazole-4,7-diyl)bis-2-thiophene-carboxaldehyde (**5**)

Compound **5** was prepared from the reaction of **3** with DMF and $POCl_3$ in 1,2-dichloroethane.[57]

4,7-Bis[α-(*p*-bromophenyl)-2-thiopheneacrylonitrile]-2,1,3-benzothiadiazole (**6**)

A flask was charged with a solution of **5** (0.50 g, 1.40 mmol) and 4-bromophenylacetonitrile (0.55 g, 2.80 mmol) in anhydrous ethanol (25 mL). Sodium hydroxide (0.12 g, 2.94 mmol) dissolved in anhydrous ethanol was added portion-wise to the stirred solution under N_2. Stirring of the mixture was continued at ambient temperature in a stream of N_2 overnight. The purple precipitate was filtered, washed thoroughly with water, and dried to afford **6** (0.18 g, 18%, mp 200–202°C).

FTIR (KBr, cm^{-1}): 3100, 3042, 2208, 1588, 1486, 1438, 1402, 1346, 1272, 1200, 1076, 1048, 1008, 822, 704, 528.

^{1}H-NMR ($CDCl_3$, ppm) [Fig. 1(a)]: 7.69 (m, 2H, benzothiadiazole protons labeled "a"); 7.52-7.43 (m, 2H, olefinic protons "c"); 7.28-7.05 (m, 12H, phenylene and thiophene protons "b").

^{13}C-NMR ($CDCl_3$, ppm) [Fig. 1(b)]: 154.1, 143.2, 137.4, 135.7, 133.6, 131.4, 129.7, 128.5, 128.3, 127.9, 127.7, 122.4, 118.7, 105.4.

Anal. Calcd. for $C_{32}H_{16}Br_2N_4S_3$: C, 53.94; H, 2.26; N, 7.86. Found: C, 53.17; H, 2.38; N, 7.62.

Preparation of copolymers

Copolymer **S**

The preparation of **S** is given as a typical example for the preparation of copolymers. A flask was charged with a mixture of **4** (0.1567 g, 0.3420 mmol), 1,4-divinyl-2,5-bis(hexyloxy)-benzene (0.1130 g, 0.3420 mmol), $Pd(OAc)_2$ (0.0032 g, 0.0143 mmol),

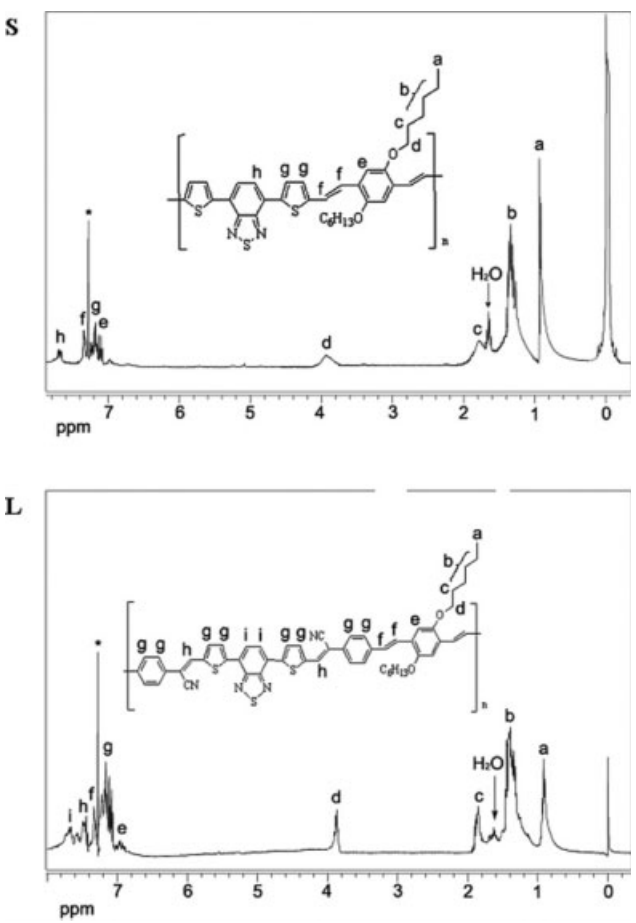

Figure 3 ^{1}H-NMR spectra in $CDCl_3$ solution of copolymers **S** (top) and **L** (bottom). The solvent peak is denoted by an asterisk.

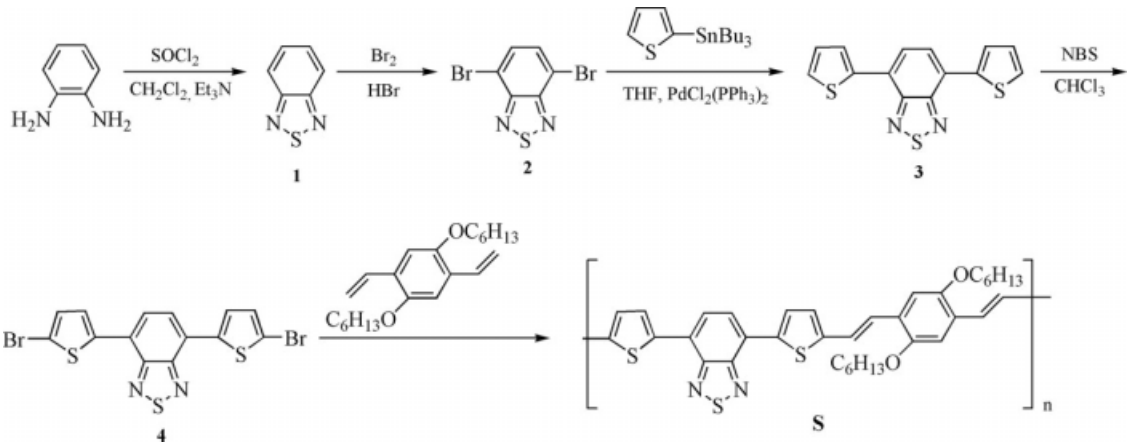

Scheme 1 Synthesis of monomers **1–4** and copolymer **S**.

P(*o*-tolyl)$_3$ (0.0239 g, 0.0785 mmol), DMF (7 mL), and triethylamine (3 mL). The flask was degassed and purged with N_2. The mixture was heated at 90°C for 24 h under N_2. Then, it was filtered and the filtrate was poured into methanol. The purple precipitate was filtered and washed with methanol. The crude product was purified by dissolving in THF and precipitating into methanol (0.19 g, 89%).

FTIR (KBr, cm^{-1}) [Fig. 2(a)]: 3100, 2926, 2866, 1654, 1458, 1420, 1180, 1036, 965, 834, 704, 512.

^{1}H-NMR ($CDCl_3$, ppm) [Fig. 3(a)] 7.65 (m, 2H, aromatic "h"); 7.32 (m, 4H, olefinic "f"); 7.18 (m, 4H, aromatic "g"); 7.10 (m, 2H, aromatic "e"); 3.94 (broad, 4H, aliphatic "d"); 1.78 (broad, 4H, aliphatic "c"); 1.34 (m, 12H, aliphatic "b"); 0.94 (t, J = 7.3 Hz, 6H, aliphatic "a").

Anal. Calcd. for $C_{36}H_{38}N_2O_2S_3$: C, 68.97; H, 6.11; N, 4.47. Found: C, 68.05; H, 6.04; N, 4.23.

Copolymer **L**

Copolymer **L** was similarly prepared in 82% yield from the reaction of **6** with 1,4-divinyl-2,5-bis(hexyloxy)-benzene.

FTIR (KBr, cm^{-1}) [Fig. 2(b)] 2936, 2882, 2209, 1660, 1450, 1392, 1172, 1036, 995, 702.

^{1}H-NMR ($CDCl_3$, ppm) [Fig. 3(b)] 7.68 (m, 2H, aromatic "i"); 7.44 (m, 2H, olefinic "h"); 7.34 (m, 4H, olefinic "f"); 7.19-7.07 (m, 12H, aromatic "g"); 6.96 (m, 2H, aromatic "e"); 3.88 (m, 4H, aliphatic "d"); 1.88 (m, 4H, aliphatic "c"); 1.41 (m, 12H, aliphatic "b"); 0.92 (t, J = 7.3 Hz, 6H, aliphatic "a").

Anal. Calcd. for $C_{54}H_{48}N_4O_2S_3$: C, 73.60; H, 5.49; N, 6.36. Found: C, 72.98; H, 5.87; N, 6.12.

Preparation of photovoltaic devices

PSCs were fabricated in the following steps. ITO glass was cleaned by detergent and acetone and treated in boiled H_2O_2. A thin PEDOT : PSS (~ 40 nm, by Veeco DEKTAK 150 surface profilometer) layer was spin coated on cleaned ITO and annealed at 120°C for 20 min on a hot plate. Then the active layers (about 70 nm) were spin coated from chlorobenzene (CB) solution. Finally, The cathode of LiF (0.6 nm)/Al (80 nm) was thermally deposited to finish the device fabrication. The device area is 5.5 mm^2. Afterwards, the devices with **S** : PCBM and **L** : PCBM active layers were annealed at 120°C for 5 min in N_2 before measurement. Current-voltage *(J-V)* characteristics were recorded by using Keithley 2400 Source Meter in the dark and under one sun of AM1.5 illumination by Solar Simulators (SCIENCETECH SS-0.5K). All fabrication and characterizations were performed in an ambient environment.

RESULTS AND DISCUSSION

Synthesis and characterization

Copolymers **S** and **L** were prepared by the reaction sequences, which are presented in Schemes 1 and 2. Compounds **1**,[55] **2**,[55] **3**,[34] **4**,[56] and **5**[57] were

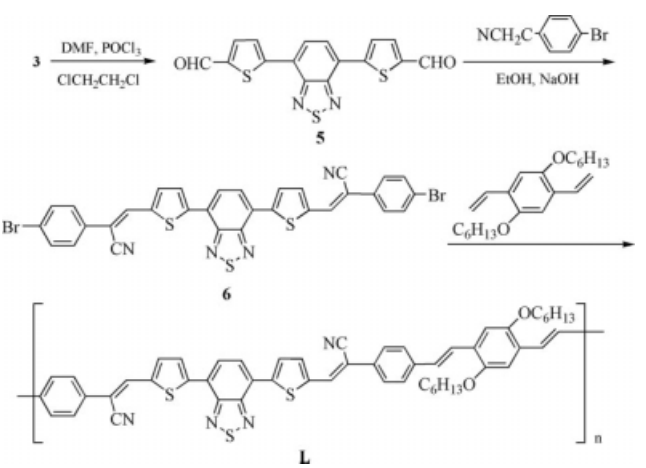

Scheme 2 Synthesis of monomers **5, 6**, and copolymer **L**.

TABLE I
Molecular Weights, Thermal, and Optical Properties of Copolymers

Sample	S	L
M_n [a]	8700	11,500
M_w/M_n [a]	1.8	2.3
M_w/M_n [a]	1.8	2.3
T_d [b] (°C)	469	540
Y_c [c] (%)	52	66
$\lambda_{a,max}$ [d] in solution (nm)	312, 453	308, 390, 477
$\lambda_{f,max}$ [e] in solution (nm)	551	580
$\lambda_{a,max}$ [d] in thin film (nm)	312, 447	312, 406, 502
$\lambda_{f,max}$ [e] in thin film (nm)	588	661
E_g^{opt} [f]	2.00 eV (618 nm) [g]	1.96 eV (634 nm)[g]

The PL emission spectra were recorded at 450 nm excitation wavelength.

[a] Molecular weights determined by GPC using polystyrene standard.

[b] Decomposition temperature corresponding to 5% weight loss in N_2 determined by TGA.

[c] Char yield at 800°C in N_2 determined by TGA.

[d] $\lambda_{a,max}$: the absorption maxima from the UV-vis spectra in THF solution or in thin film.

[e] $\lambda_{f,max}$: the PL maxima in THF solution or in thin film.

[f] E_g: The optical band gap calculated from the onset of the thin film absorption.

[g] Numbers in parentheses indicate the thin film absorption onset.

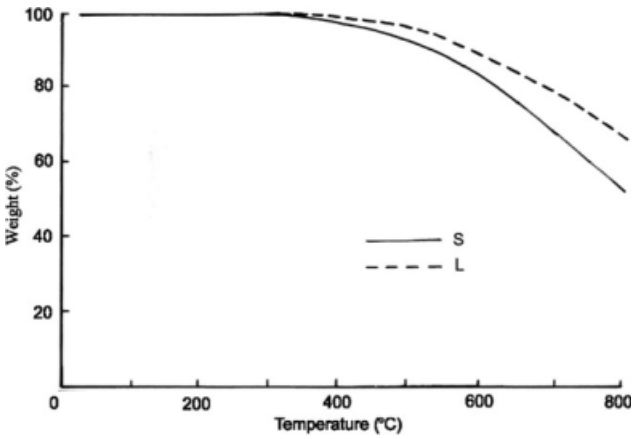

Figure 4 TGA thermograms of copolymers **S** and **L**. Conditions: N_2 flow, 60 cm^3/min, heating rate, 20°C/min.

synthesized according to the literature. Moreover, 1,4-divinyl-2,5-bis(hexyloxy)-benzene[54] was synthesized by Stille reaction[53] of 1,4-dibromo-2,5-bis-(hexyloxy)-benzene with tri-*n*-butyl(vinyl)tin. The synthesis of **6** has not been previously reported and it was achieved from the reaction of **5** with 4-bromophenylacetonitrile in anhydrous ethanol in the presence of sodium hydroxide. Compound **6** precipitated as purple solid from the reaction mixture. *tert*-BuOK could be used instead of sodium hydroxide. Finally, the Heck[58] coupling of 1,4-divinyl-2,5-bis(hexyloxy)-benzene with dibromides **4** and **6** afforded the copolymers **S** and **L**, respectively. They were very soluble in THF, chloroform, dichloromethane, toluene, and other common organic solvents owing to the presence of the hexyloxy side groups. These copolymers were purified by dissolution in THF and precipitation into methanol. The number-average molecular weights (M_n) of **S** and **L**, which were determined by GPC, were 8700 and 11,500 with polydispersity of 1.8 and 2.3, respectively (Table I). The Heck reaction usually gives polymers with relatively low molecular weights.[59]

Structural characterization of the key-dibromide **6** was accomplished by FTIR, ^{1}H-NMR [Fig. 1(a)], and ^{13}C-NMR spectroscopy [Fig. 1(b)]. Figures 2 and 3 present the FTIR and 1H-NMR spectra of copolymers,

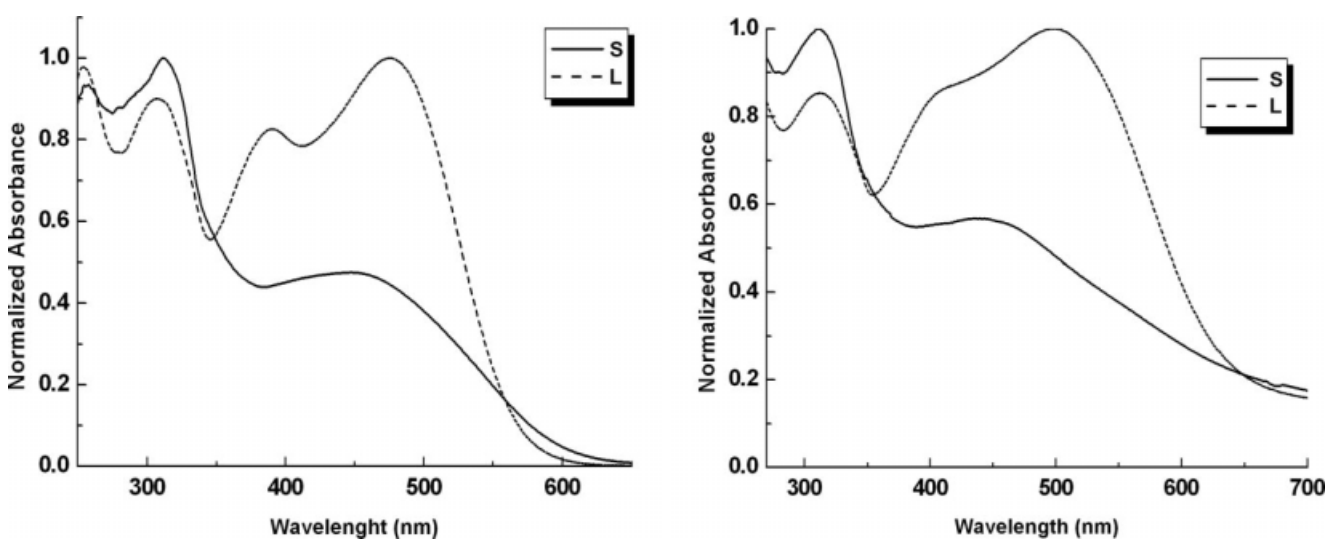

Figure 5 Normalized UV-vis absorption spectra of copolymers **S** and **L** in THF solution (a) and thin film (b).

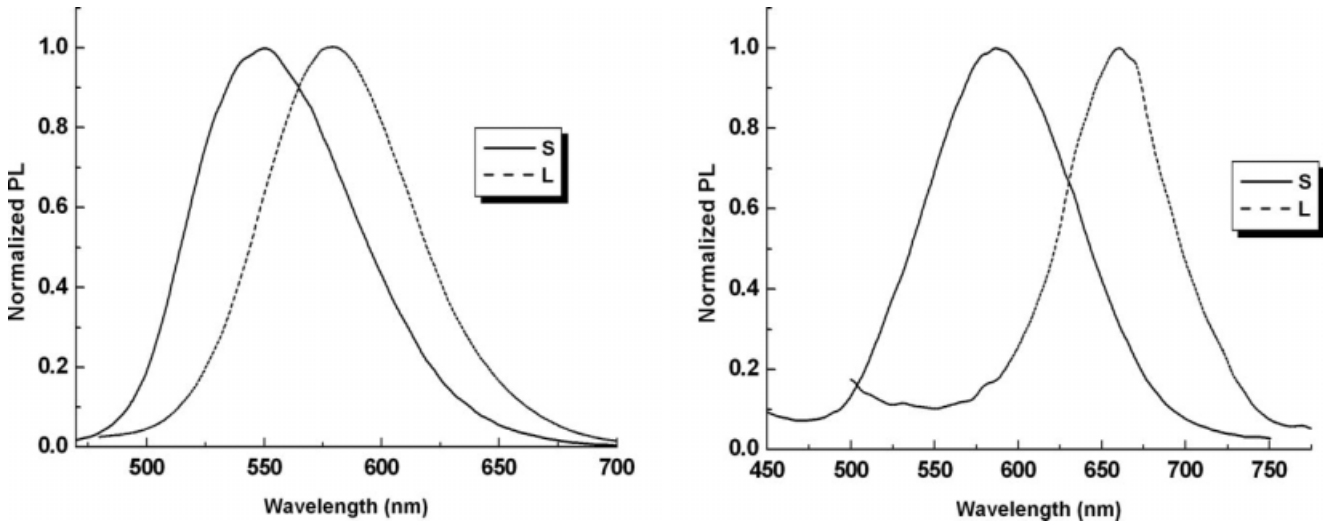

Figure 6 Normalized PL emission spectra of copolymers **S** and **L** in THF solution (a) and thin film (b). The PL emission spectra were recorded using the maximum excitation wavelength (450 nm).

which were consistent with their chemical structures. Copolymer **S** [Fig. 2(a)] showed characteristic absorption bands at 2926, 2866 (C—H stretching of aliphatic chains); 3100, 1458 (aromatic); 1654, 1420, 834, 704 (benzothiadiazole and thiophene rings); 1180, 1036 (ether bond); and 965 cm^{-1} (trans olefinic bond). Besides the absorptions at these spectrum regions, copolymer **L** [Fig. 2(b)] displayed absorption at 2209 cm^{-1} associated with the cyano group.

The ^{1}H-NMR spectrum of **S** [Fig. 3(a)] showed an upfield signal at 7.65 ppm assigned to the benzothiadiazole protons labeled "h." The olefinic protons "f," the thiophene protons "g," and the aromatic protons "e" resonated at 7.32, 7.18, and 7.10 ppm, respectively. Finally, the aliphatic protons "a," "b," "c," and "d" gave signals at 0.94, 1.34, 1.78, and 3.94 ppm, respectively. Copolymer **L** [Fig. 3(b)] exhibited a comparable ^{1}H-NMR spectrum, but it was more complex than that of **S** due to the differentiation of the olefinic proton shifts. In particular, the olefinic protons "f" resonated at 7.34 ppm, while the olefinic protons "h" resonated at a higher shift of 7.44 ppm, because of the electron-withdrawing cyano group.

The thermal stability of copolymers was evaluated by TGA in N_2 (Fig. 4). Their decomposition temperature (T_d) and the char yield (Y_c) at 800°C are listed in Table I. Copolymer **L** showed a slightly higher thermal stability than **S** due to the lower content of the hexyloxy groups per repeating unit. Generally, the copolymers were stable up to about 350°C, had T_d of 469–540°C, and Y_c of 52–66%.

Photophysical properties

The normalized UV-vis absorption spectra (Fig. 5) and PL emission spectra (Fig. 6) of copolymers **S** and **L** in both dilute (10^{-5} M) THF solution and thin film were recorded. All the spectroscopic data are summarized in Table I.

The absorption spectra of **S** (Fig. 5) showed two maxima ($\lambda_{a,max}$) at 312 and ~ 450 nm in solution and thin film. The absorption spectra of **L** were similar with three $\lambda_{a,max}$ at 308, 390, and 477 nm in solution and 312, 406, and 502 nm in thin film. The $\lambda_{a,max}$ at shorter wavelength (below 450 nm) are attributable to the n-π* transitions, while the $\lambda_{a,max}$ at longer wavelengths (above 450 nm) correspond to the π−π* transition of the copolymer backbone. The longer wavelength absorption peak of **L** in both solution and thin film is significantly more intense than that of **S**. Copolymer **S** had the most blue-shifted $\lambda_{a,max}$ at longer wavelength (453 and 447 nm) between the two copolymers, suggesting increased disruption of π-conjugation. **L** had the most red-shifted $\lambda_{a,max}$ at longer wavelength (477 and 502 nm), indicating relatively

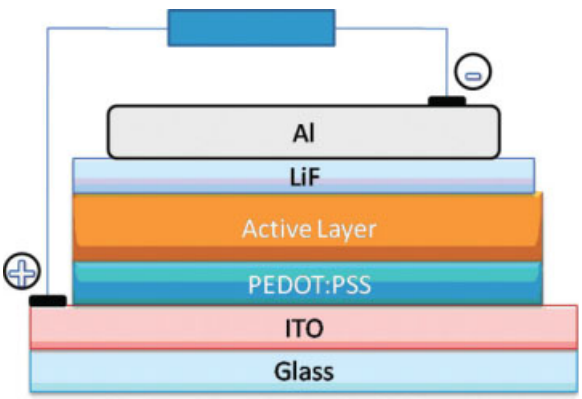

Scheme 3 Schematic structure of the devices. [Color figure can be viewed in the online issue, which is available at www.interscience.wiley.com.]

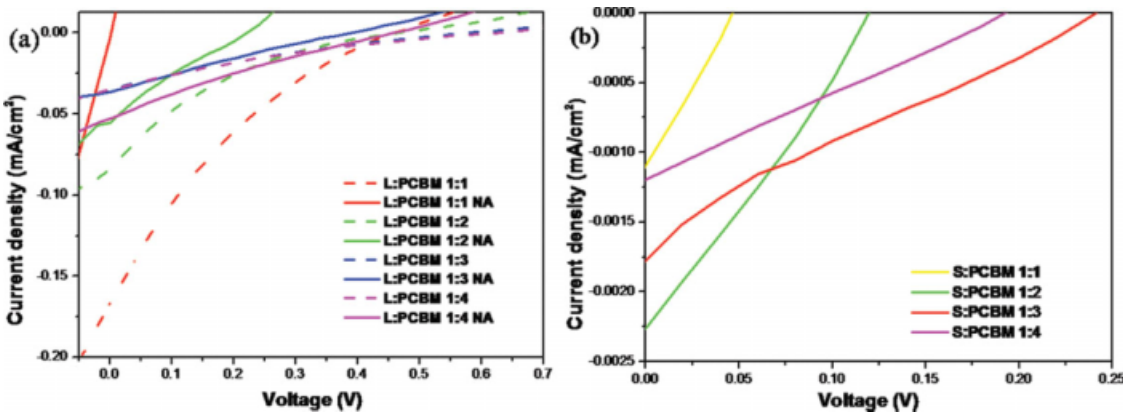

Figure 7 Current-density (J) versus voltage (V) curves of the devices with blend films (a) **L** : PCBM and (b) **S** : PCBM under one sun of AM1.5 illumination by Solar Simulators (SCIENCETECH SS-0.5K). [Color figure can be viewed in the online issue, which is available at www.interscience.wiley.com.]

longer conjugation length. The elongation of the repeating unit of **L** by inserting two additional phenylene rings and two cyano-substituted vinylene bonds relative to **S** should be responsible for this behavior. The absorption onset in thin film of copolymers **S** and **L** were 618 and 634 nm, from which the optical band gaps (E_g^{opt}) of the copolymers were determined to be 2.00 and 1.96 eV, respectively. The E_g^{opt} of the present copolymers is lower than that of MEH-PPV60 (2.10 eV). PPV-copolymers derived from 1-methoxy-4-octyloxyphenylene, 2,1,3-benzothiadiazole, and trans-1,2-bis(tributylstannyl)ethylene[60] had E_g^{opt} of 2.12–1.78 eV. Finally, a E_g^{opt} of 1.94 eV has been reported for poly[(dioctyloxyphenylene ethynylene)-*alt*-(2,1,3-benzothiadiazole)].[61]

By photoexcitation at 450 nm, the copolymers emitted yellow light in solution and orange-red light in thin film (Fig. 6). The emission maximum ($\lambda_{f,max}$) of **S** was located at 551 nm in solution and 588 nm in thin film. Again, the $\lambda_{f,max}$ of **L** was red-shifted relative to **S** and was located at 580 nm in solution and 661 nm in thin film. This supports that the color of the emitted light could be tuned by elongation of the repeating unit.

Photovoltaic properties

Photovoltaic properties of devices with active layers containing 50, 67, 75, 80 wt % PCBM in **S** and **L** was investigated. Optimization of film composition and morphology and the thermal annealing treatment strategies ware done to optimize the performance of the devices. To investigate the photovoltaic properties of the **S** and **L** compounds, as shown in Scheme 3, solar cells with a structure of ITO/PEDOT-PSS/compound **S** (or **L**) : PCBM/LiF/Al were fabricated. The compounds **S** and **L** were used as donor and PCBM as acceptor. The active layers were prepared by spin-coating the blend solution of the compounds and PCBM with weight ratio from 1 : 1 to 1 : 4. The current-density (J) versus voltage (V) curves of the devices are shown in Figure 7. All of the device parameters (PCE, V_{OC}, J_{SC}, FF) are summarized in Table II. Through thermal annealing at 120°C for 5 min, the V_{oc} of all devices decreased. The device based on **S** : PCBM had a PCE almost 0% after annealing. For devices based on **L** : PCBM, the best device performance was obtained at a ratio of 1 : 1 (L : PCBM) with J_{SC} = 0.17 mA/cm^2, V_{OC} = 0.45, FF = 0.18, and PCE = 0.014%, but all parameters decrease to 0 after annealing. So for the devices based on **S** and **L**, the annealing process could lead to a decrease of the photovoltaic properties. The results quite differ from the case in P3HT : PCBM. Much research has been shown independently to have a positive effect on solar cell performance with the thermal treatment.[62–64]

We have investigated the morphology of the blend films with 50, 67, 75, 80 wt % PCBM in **S** and **L**.

TABLE II
Short-Circuit Current (J_{SC}), Open Circuit-Voltage (V_{OC}), Fill Factor (FF), and Power Conversion Efficiency (PCE) as a Function of Annealing and for the PV Devices Based on S (or L) : PCBM with Different PCBM Concentrations

Sample : PCBM (w : w)	Annealing (120°C)	J_{sc} (mA/cm^2)	FF (%)	V_{oc} (V)	PCE (%)
L : PCBM (1 : 1)	5 min	0	0	0	0
L : PCBM (1 : 1)	None	0.17	18	0.45	0.014
L : PCBM (1 : 2)	5 min	0.06	21	0.22	0.003
L : PCBM (1 : 2)	None	0.08	14	0.45	0.005
L : PCBM (1 : 3)	5 min	0.04	22	0.40	0.004
L : PCBM (1 : 3)	None	0.04	19	0.58	0.004
L : PCBM (1 : 4)	5 min	0.04	21	0.45	0.004
L : PCBM (1 : 4)	None	0.05	17	0.58	0.005
S : PCBM (1 : 1)	None	0.001	30	0.04	$1.2*10^{-5}$
S : PCBM (1 : 2)	None	0.002	28	0.12	$6.7*10^{-5}$
S : PCBM (1 : 3)	None	0.002	23	0.24	$1.2*10^{-4}$
S : PCBM (1 : 4)	None	0.001	24	0.20	$4.8*10^{-5}$

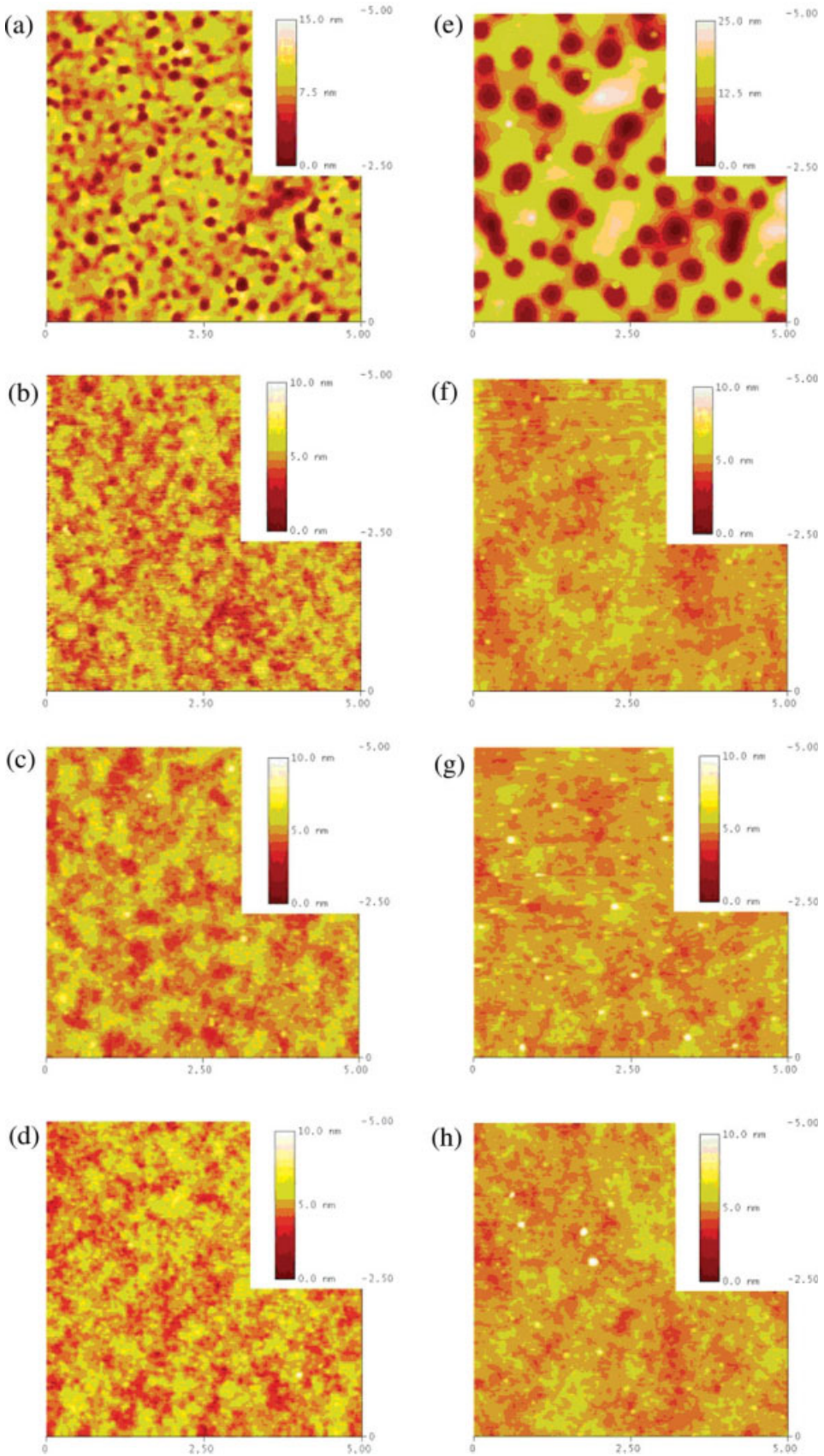

Figure 8 AFM image of the blend film of **S** : PCBM with different PCBM concentrations before (a-d) and after (e-h) thermal annealing treatment. [Color figure can be viewed in the online issue, which is available at www.interscience.wiley.com.]

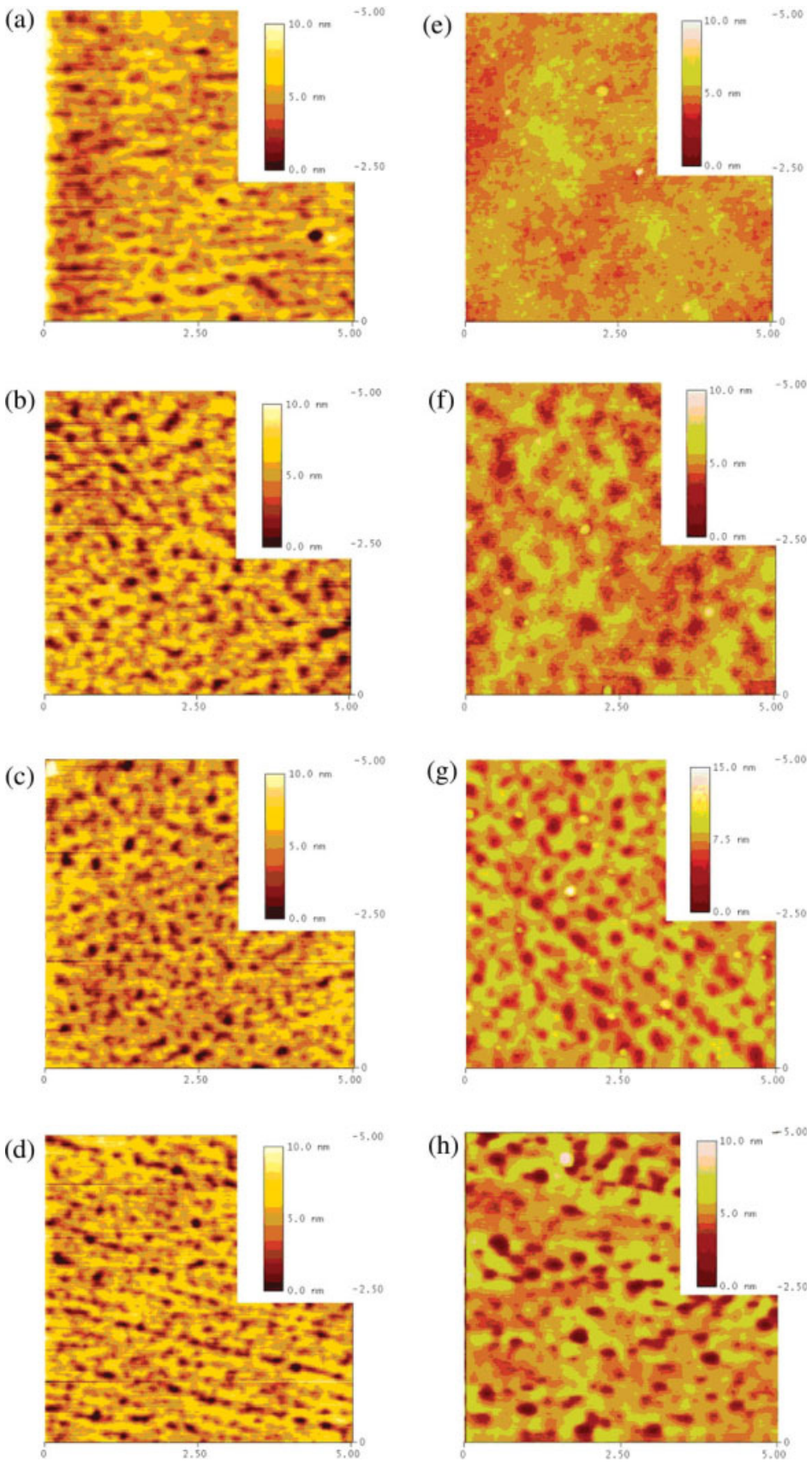

Figure 9 AFM image of the blend film of **L** : PCBM with different PCBM concentrations before (a-d) and after (e-h) thermal annealing treatment. [Color figure can be viewed in the online issue, which is available at www.interscience.wiley.com.]

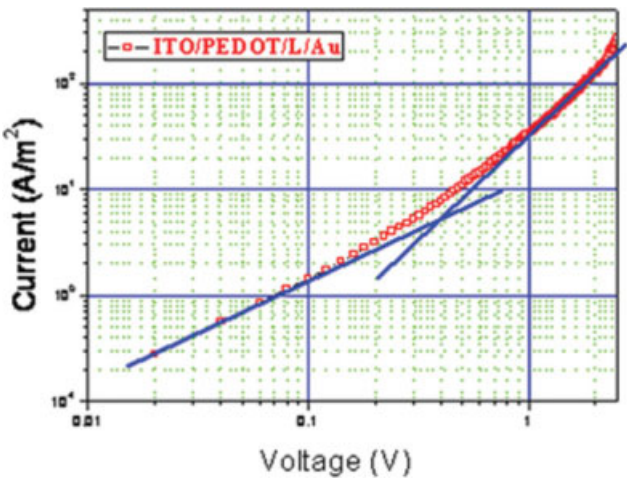

Figure 10 $J-V$ curve in the dark of an ITO/PEDOT/**L**/Au device in log axis for estimating the hole mobility of **L**. The thickness of **L** is around 50 nm. The open rectangle symbols are the experimental data. The solid line from 0.01 to 0.40 V means log J is fitted linearly dependent on log V with a slope of 1. The solid line from 0.4 to 1 V log J is fitted linearly dependent on log V with a slope of 2 (SCLC area). [Color figure can be viewed in the online issue, which is available at www.interscience.wiley.com.]

They have been studied by AFM before and after thermal annealing at 120°C for 5 min.

As shown in Figure 8, for the blend films with 50, 67, 75, 80 wt % PCBM in **S** before annealing, the RMS were 1.7, 0.7, 0.5, and 0.7 nm, respectively, and the relative high current densities obtained for the 75 wt % PCBM composition film in **S**, which has the lowest RMS. The smooth surface of the blend film ensures better contact with the LiF/Al electrode, which is also helpful to the increase of carrier collection efficiency. After annealing the blend film with 50 wt % PCBM shows significant phase separation. That is why the PCE decrease dramatically after annealing.

As shown in Figure 9, for the blend films with 50, 67, 75, 80 wt % PCBM in **L**, the RMS were 1.2, 1.6, 1.5, and 1.3 nm before annealing, and after annealing the RMS were 0.3, 0.6, 0.9, and 1.1 nm, respectively. Photovoltaic performance of the blend film with 50 wt % PCBM in **L** with RMS of 1.2 nm showed the highest PCE.

Previously Colladet et al.[65] and Thompson et al.[66] reported cyano-vinylene containing polymers as donors and PCBM as acceptor for PSCs. Their PCE are about 0.1%, which is possibly due to the low hole mobility in these polymers.

We estimated the hole mobility of **L** approximately by the space charge limited current (SCLC) methods.[67] Devices with a structure of ITO/PEDOT/**L**/Au were fabricated. Their J-V curves in the dark are shown in Figure 10. It can be seen that in low-voltage area (from 0.01 to 0.40 V) log J is linearly dependent on log V with a slope of 1. In a relatively high-voltage area (from 0.4 to 1V) log J can also be fitted to be linearly dependent on log V and the slope is 2. The J-V in this high-voltage area is corresponding to the SCLC behavior. The work function of ITO/PEDOT is about −5.2 eV and that of Au is about −5.0 eV. We estimated the hole mobility of **L** according to the equation:

$$J = \frac{9}{8}\varepsilon_r\varepsilon_0\mu_h\frac{(V - V_{bi})^2}{L^3}$$

where V is the applied voltage, J is the current density, ε_r and ε_0 are the relative dielectric constant and the permittivity of the free space (8.85×10^{-12} F/m), respectively, μh is electron mobility, and **L** is the thickness of the organic layer. Here we fit ε_r to be 3. V_{bi} is fitted to be about 0.2 V, which is determined by the difference between the work functions of cathode and anode. Then the hole mobility of **L** is estimated to be about 1.639×10^{-6} $cm^2V^{-1}S^{-1}$ and the low PCEs could be probably due to the low hole mobility.

CONCLUSIONS

The alternating phenylenevinylene copolymers **S** and **L** were prepared by Heck reaction of 1,4-divinyl-2,5-bis(hexyloxy)-benzene with dibromides **4** and **6**, respectively. They contained dithienbenzothiadiazole (acceptor) and dihexyloxybenzene (donor) moieties. The copolymers dissolved in common organic solvents were stable up to about 350°C and afforded char yields of 52–66% at 800°C in N_2. The absorption spectra showed a longer wavelength maximum at 447–502 nm and optical band gap of ~ 2.0 eV. The copolymers emitted yellow light in solution and orange-red light in thin film. The emission maximum of **L** was red-shifted as compared to **S**. In PSCs based on **S** (or **L**), PCBM exhibit a low PCE under one sun of AM1.5 illumination by Solar Simulators, which is possibly due to the low hole mobility in these polymers.

References

1. Kim, J. Y.; Kim, S. H.; Lee, H.-H.; Lee, K.; Ma, W.; Gong, X.; Heeger, A. J. Adv Mater (Weinheim, Germany) 2006, 18, 572.
2. Reyes, R. M.; Kim, K.; Carroll, D. J Appl Phys Lett 2005, 87, 083506.
3. Kim, Y.; Cook, S.; Tuladhar, S. M.; Choulis, S. A.; Nelson, J.; Durrant, J. R.; Bradley, D. D. C.; Giles, M.; Mcculloch, I.; Ha, C. S.; Ree, M. Nat Mater 2006, 5, 197.
4. Li, G.; Shrotriya, V.; Huang, J.; Yao, Y.; Moriarty, T.; Emery, K.; Yang, Y. Nat Mater 2005, 4, 864.
5. Li, G.; Shortriya, V.; Yao, Y.; Yang, Y. J Appl Phys 2005, 98, 043704/1.
6. Chirvase, D.; Parisi, J.; Hummelen, J. C.; Dyakonov, V. Nanotechnology 2004, 15, 1317.

7. De Bettignies, R.; Leroy, J.; Firon, M.; Sentein, C. Synth Met 2006, 156, 510.
8. Mihailetchi, V. D.; Xie, H.; de Boer, B.; Popescu, L. M.; Hummelen, J. C.; Blom, P. W. M.; Koster, L. J. A. Appl Phys Lett 2006, 89, 012107/1.
9. Mihailetchi, V. D.; Xie, H.; de Boer, B.; Koster, L. J. A.; Blom, P. W. M. Adv Funct Mater 2006, 16, 699.
10. Chang, E. C.; Chen, S. A. J Appl Phys 1999, 85, 2057.
11. Jang, M. S.; Song, S. Y.; Shim, H. K. Polymer 2000, 41, 5675.
12. Peres, L. O.; Fernandes, M. R.; Garcia, J. R.; Wang, S. H.; Nart, F. C. Synth Met 2006, 156, 529.
13. Gurge, R. M.; Sarker, A.; Lahti, P. M.; Hu, B.; Karasz, F. E. Macromolecules 1997, 30, 8286.
14. Jin, J. I.; Kim, J. C.; Shim, H. K. Macromolecules 1992, 25, 5519.
15. Samal, G. S.; Biswas, A. K.; Singh, S.; Mohapatra, Y. N. Synth Met 2005, 155, 303.
16. Lahti, P. M.; Sarker, A.; Garay, R. O.; Lenz, R. W.; Karasz, F. E. Polymer 1994, 35, 1312.
17. Grimsdale, A. C.; Cacialli, F.; Gruener, J.; Li, X.-C.; Holmes, A. B.; Moratti, S. C.; Friend, R. H. Synth Met 1996, 76, 165.
18. Boardman, F. H.; Grice, A. W.; Ruether, M. G.; Sheldon, T. J.; Bradley, D. D. C.; Burn, P. L. Macromolecules 1999, 32, 111.
19. Jin, Y.; Ju, J.; Kim, J.; Lee, S.; Kim, J. Y.; Park, S. H.; Son, S.-M.; Jin, S.-H.; Lee, K.; Suh, H. Macromolecules 2003, 36, 6970.
20. Greenham, N. C.; Moratti, S. C.; Bradley, D. D. C.; Friend, R. H.; Holmes, A. B. Nature (London) 1993, 365, 628.
21. Bröms, P.; Birgersson, J.; Johansson, N.; Lögdlund, M.; Salaneck, W. R. Synth Met 1995, 74, 179.
22. Lux, A.; Holmes, A. B.; Cervini, R.; Davies, J. E.; Moratti, S. C.; Gruener, J.; Cacialli, F.; Friend, R. H. Synth Met 1997, 84, 293.
23. Jin, Y.; Kim, J.; Lee, S.; Kim, J. Y.; Park, S. H.; Lee, K.; Suh, H. Macromolecules 2004, 37, 6711.
24. Yu, G.; Heeger, A. J. J Appl Phys 1995, 78, 4510.
25. Veenstra, S. C.; Verhees, W. J. H.; Kroon, J. M.; Koetse, M. M.; Sweelssen, J.; Bastiaansen, J. J. A. M.; Schoo, H. F. M.; Yang, X.; Alexeev, A.; Loos, J.; Schubert, U. S.; Wienk, M. M. Chem Mater 2004, 16, 2503.
26. Breeze, A. J.; Schlesinger, Z.; Carter, S. A.; Tillmann, H.; Horhold, H.-H. Sol Energy Mater Sol Cells 2004, 83, 263.
27. Kietzke, T.; Hoerhold, H.-H.; Neher, D. Chem Mater 2005, 17, 6532.
28. Brabec, C. J.; Sariciftci, N. S.; Hummelen, J. C. Adv Funct Mater 2001, 11, 15.
29. Jenekhe, S. A.; Yi, S. Appl Phys Lett 2000, 77, 2635.
30. Thompson, B. C.; Frechet, J. M. J. Angew Chem Int Ed 2008, 47, 58.
31. Winder, C.; Sariciftci, N. S. J Mater Chem 2004, 14, 1077.
32. Yu, W.-L.; Meng, H.; Pei, J.; Huang, W. J Am Chem Soc 1998, 120, 11808.
33. Van De Wetering, K.; Brochon, C.; Ngov, C.; Hadziioannou, G. Macromolecules 2006, 39, 4289.
34. Kitamura, C.; Tanaka, S.; Yamashita, Y. Chem Mater 1996, 8, 570.
35. Yamamoto, T.; Zhou, Z.; Kanbara, T.; Shimura, M.; Kizu, K.; Maruyama, T.; Nakamura, Y.; Fukuda, T.; Lee, B.-L. J Am Chem Soc 1996, 118, 10389.
36. Zhang, Q. T.; Tour, J. M. J Am Chem Soc 1998, 120, 5355.
37. Lee, B.-L.; Yamamoto, T. Macromolecules 1999, 32, 1375.
38. Dhanabalan, A.; van Dongen, J. L. J.; van Duren, J. K. J.; Janssen, H. M.; van Hal, P. A.; Janssen, R. A. J. Macromolecules 2001, 34, 2495.
39. Svensson, M.; Zhang, F.; Veenstra, S. C.; Verhees, W. J. H.; Hummelen, J. C.; Kroon, J. M.; Inganaes, O.; Andersson, M. R. Adv Mater 2003, 15, 988.
40. Campos, L. M.; Tontcheva, A.; Guenes, S.; Sonmez, G.; Neugebauer, H.; Sariciftci, N. S.; Wudl, F. Chem Mater 2005, 17, 4031.
41. Thompson, B. C.; Kim, Y.-G.; Reynolds, J. R. Macromolecules 2005, 38, 5359.
42. Bundgaard, E.; Krebs, F. C. Macromolecules 2006, 39, 2823.
43. Roncali, J. Chem Rev (Washington, DC) 1997, 97, 173.
44. Roncali, J. Macromol Rapid Commun 2007, 28, 1761.
45. Zhou, Q.; Hou, Q.; Zheng, L.; Deng , X.; Yu, G.; Cao, Y. Appl Phys Lett 2004, 84, 1653.
46. Wong, W.-Y.; Choi, K.-H.; Lu, G.-L.; Shi, J.-X. Macromol Rapid Commun 2001, 22, 461.
47. Akoudad, S.; Roncali, J. Chem Commun (Cambridge) 1998, 19, 2081.
48. Raimundo, J.-M.; Blanchard, P.; Brisset, H.; Akoudad, S.; Roncali, J. Chem Commun (Cambridge) 2000, 11, 939.
49. Perepichka, I. F.; Perepichka, D. F.; Meng, H.; Wudl, F. Adv Mater (Weinheim, Germany) 2005, 17, 2281.
50. Fichou, D.; Ziegler, C. Handbook of Oligo- and Polythiophenes; Wiley-VCH: Weinheim, Germany, 1999; pp 183–282.
51. Stott, T. L.; Wolf, M. O. Coord Chem Rev 2003, 246, 89.
52. Xia, Y.; Luo, J.; Deng, X.; Li, X.; Li, D.; Zhu, X.; Yang, W.; Cao, Y. Macromol Chem Phys 2006, 207, 511.
53. McKean, D. R.; Parrinello, G.; Renaldo, A. F.; Stille, J. K. J Org Chem 1987, 52, 422.
54. Peng, Q.; Li, M.; Tang, X.; Lu, S.; Peng, J.; Cao, Y. J Polym Sci Part A: Polym Chem 2007, 45, 1632.
55. Mancilha, F. S.; Da Silveira Neto, B. A.; Lopes, A. S.; Moreira, P. F., Jr.; Quina, F. H.; Goncalves, R. S.; Dupont, J. Eur J Org Chem 2006, 21, 4924.
56. Li, X.; Zeng, W.; Zhang, Y.; Hou, Q.; Yang, W.; Cao, Y. Eur Polym J 2005, 41, 2923.
57. Zhang, X.; Yamaguchi, R.; Moriyama, K.; Kadowaki, M.; Kobayashi, T.; Ishi-i, T.; Thiemann, T.; Mataka, S. J Mater Chem 2006, 16, 736.
58. Ziegler, C. B., Jr.; Heck, R. F. Org Chem 1978, 43, 2941.
59. Hilberer, A.; Brouwer, J.-H.; Van der Scheer, B. J.; Wildeman, J.; Hadziioannou, G. Macromolecules 1995, 28, 4525.
60. Li, X.; Zhang, Y.; Yang, R.; Huang, J.; Yang, W.; Cao, Y. J Polym Sci Part A: Polym Chem 2005, 43, 2325.
61. Lu, S.; Yang, M.; Luo, J.; Cao, Y.; Bai, F. Macromol Chem Phys 2005, 206, 664.
62. Kim, Y.; Choulis, S. A.; Nelson, J.; Bardley, D. D. C. Appl Phys Lett 2005, 86, 063502/1.
63. Zen, A.; Pflaum, J.; Hirschmann, S.; Zhuang, W.; Jaiser, F.; Asawapirom, U.; Rabe, J. P.; Scherf, U.; Neher, D. Adv Funct Mater 2004, 14, 757.
64. Li, G.; Shrotriya, V.; Yao, Y.; Huang, J. S.; Yang, Y. J Mater Chem 2007, 17, 3126.
65. Colladet, K.; Fourier, S.; Cleij, T. J.; Lutsen, L.; Gelan, J.; Vanderzande, D.; Nguyen, L. H.; Neugebauer, H.; Sariciftci, S.; Aguirre, A.; Janssen, G.; Goovaerts, E. Macromolecules 2007, 40, 65.
66. Thompson, B. C.; Kim, Y. G.; Mccarley, T. D.; Reynolds, J. R. J Am Chem Soc 2006, 128, 12714.
67. Blom, P. W. M.; deJong, M. J. M.; vanMunster, M. G. Phys Rev B 1997, 55, R656.